



ELSEVIER

Available online at www.sciencedirect.com

SCIENCE @ DIRECT®

Optics Communications 223 (2003) 67–74

OPTICS
COMMUNICATIONS

www.elsevier.com/locate/optcom

A feedback-injected Fabry–Perot laser diode filtering technique for side-mode suppression and linewidth reduction of erbium-doped fiber lasers

Gong-Ru Lin*, Shih-Kai Lee

Institute of Electro-Optical Engineering, National Chiao Tung University, 1001 Ta Hseuh Rd., Hsinchu 300, Taiwan, ROC

Received 14 January 2003; received in revised form 22 May 2003; accepted 4 June 2003

Abstract

By adding a fiber-pigtailed Fabry–Perot laser diode (FPLD) into a close-loop erbium-doped fiber amplifier (EDFA) ring cavity, and feedback-injecting the FPLD biased at just below threshold and the EDFA each other via directional couplers, we demonstrate a low-cost band-pass filtering technique for constructing narrow linewidth erbium-doped fiber laser (EDFL) with ultrahigh side-mode suppression ratio (SMSR). Under an output coupling ratio of 90%, the mutually injection-locked EDFL–FPLD link exhibits a maximum output power and SMSR of up to 98.6 mW and 49.6 dB at wavelength 1561.37 nm, respectively. Wavelength tuning of up to 6 nm can be achieved by tuning the temperature and fine adjusting the below threshold driven current of FPLD. The minimum spectral linewidth at 3dB-decay of as small as 0.017 nm measuring by commercial optical spectrum analyzer with limited resolution bandwidth of 0.01 nm are observed. The stabilities in power, SMSR, peak wavelength of ± 0.01 mW, ± 0.5 dB, and ± 0.025 nm, respectively, are also determined.

© 2003 Elsevier Science B.V. All rights reserved.

Keywords: Erbium-doped fiber laser; Fabry–Perot laser diode; Feedback-injection; Mutual injection-locking; Band-pass filter; Narrow linewidth; Side-mode suppression ratio

1. Introduction

Broadband wavelength tunable lasers with narrow linewidth and high-side-mode suppressing ratio (SMSR) are the promising optical sources for fiber-optic communication or diagnostic systems.

Typically, this requirement can be satisfied via a set of distributed Bragg reflector (DBR) or distributed feedback (DFB) laser diode (LD) array. Generally, the DFBLD exhibits a SMSR of 35–50 dB, an output power of 10s mW, and an ultranarrow linewidth of 10s MHz or less. The broadband wavelength tuning is achieved by tuning the temperature of each DFBLD operating at discrete wavelength [1]. In addition, versatile external cavity lasers using ultranarrow band-pass optical filters such as fiber Bragg grating (FBG) [2],

* Corresponding author. Tel.: +886-3-5712121x56376; fax: 886-228281873.

E-mail address: gmlin@faculty.nctu.edu.tw (G.-R. Lin).

Fabry–Perot etalon [3], and other diffraction gratings have also emerged. In particular, it was reported that a conventional Fabry–Perot laser diode (FPLD) can also be converted into a single longitudinal-mode laser source by simply injection-locking it with a single-mode coherent source or feedback seeding it with the filtered output [4,5]. Subsequently, the more complicated and less cost-effective external-feedback or self-seeding techniques [6,7] have been demonstrated with optimized SMSR of below 35 dB. However, these make the whole system expansive, bulky and complicated in alignment. The alternative single-mode lasing scheme can be achieved by self-injection seeding a FPLD with a distributed feedback output from a linearly chirped FBG band-pass filter and wavelength controller [8], or a Fabry–Perot semiconductor filter [23]. The consistent features of these schemes for LDs are their linear-cavity configurations, lower output powers (due to coupled cavity design), and relatively large linewidths.

Recently, the erbium-doped fiber laser (EDFL) has emerged as a novel optical sources due to its superior compatibility with fiber-optic networks and its widely wavelength-tuning characteristics covering C and L band. These make the EDFL as a potential source for characterization of passive fiber-optic WDM or DWDM components, generation of narrow-linewidth optical carriers for fiber sensing [9] and spectroscopy, etc. [10]. Versatile researches toward narrow linewidth EDFL based upon either linear (a Fabry–Perot scheme by embedding gratings or reflectors in the both ends of EDFL [11–14]) or ring-cavity designs (composed of two narrow-band fiber-based Fabry–Perot filters [15] or high-finesse etalons [3]) have been reported. Linear-cavity single-mode EDFL was implemented by using an EDF with intracore distributed Bragg reflectors [11–13], or gratings [14] to provide both optical feedback and wavelength selectivity. These are written by directly UV-exposing the EDF to periodically change its refractive index at both ends. The linear-cavity EDFL are compact and spectrally narrow (due to large free-spectral-range), however, such a scheme also results in a low-output power of 5 mW or less owing to the low-slope efficiency (output power/

absorbed pump power) and the short-EDF length. On the other hand, the ring-cavity single-mode EDFL is typically constructed with two high-finesse fiber Fabry–Perot filters (FFPFs) to guarantee the single-mode lasing with ultranarrow spectral linewidth from several kHz to MHz and SMSR 35 dB or higher [3,15]. The mode-linewidth of the ring-cavity EDFL system can be far smaller than that of an EDFL with linear cavity. However, the use of such FFPFs not only makes the whole system complex and expansive, but also reduces the EDFL output power to below 10 mW (due to high-insertion loss of FFPF). Furthermore, the present narrow linewidth and wavelength tunable EDFL approaches are relatively expansive as compared to the commercially available wavelength-tunable source based on DFBLD array. On the other hand, the free-running EDFL still suffers from difficulty in long-term stabilizing its lasing frequency as compared to the DFBLD. The highly sensitive nature of EDFL ring cavity with respect to environmental perturbations inevitably leads to a hopping between its longitudinal modes with small free-spectral ranges. Without self-seeding or feedback-injection control, the free-running EDFL usually exhibits a time-dependent multi-mode output with fluctuated power at peak wavelength and a relatively poor SMSR, which originates from the statistical contribution of randomly coupled spontaneous emission to each lasing mode [16]. Unless the narrow-linewidth and high-SMSR lasing properties truly achieved, the EDFL source can rarely be employed for aforementioned applications even with a spectrum-slicing and band-pass filtering technique, or with a self-feedback injecting (or so-called regenerating) scheme using the amplified spontaneous emission of the close-loop EDFA itself. More recently, a multi-loop EDFL with two piezoceramic stretchers has been developed to achieve narrow-linewidth output with higher SMSR (>40 dB) [17].

Nonetheless, the simplified approaches for narrow linewidth EDFLs with high-SMSR using easily obtainable and cost-effective components were less addressed. Among the numerous studies, it is found a distinguished approach in which the single-mode pulses can be generated by self-seeding FPLD with low-level (about 0.2–6%) feedback

power [18]. Moreover, a mutually injection-locked DFBLD-EDFL link lasing at the single longitudinal mode of DFBLD with a reduced linewidth and greatly improved side-mode suppressing ratio (SMSR) as compared to that of the DFBLD or EDFL operated in free-running condition was implemented [19]. The EDFL is forced to synchronize with the DFBLD operating at slightly above threshold condition with injection power of $29 \mu\text{W}$. By taking the self-seeding and mutual injection-locking concepts of these works, we demonstrate a narrow-linewidth and wavelength-tunable EDFL source with ultrahigh SMSR. This is implemented by combining a close-loop EDFA with an intra-cavity feedback-injected fiber-pigtailed FPLD via commercial optical couplers, the performances of such a novel EDFL source in linewidth, wavelength-tuning range, SMSR, average power, output stability, and relative-intensity noise (RIN) are discussed. The comparisons of the proposed EDFL with the free-running FPLD, the free-running EDFL, the EDFL with commercial optical band-pass filter (OBPF), and the DFBLD are reported.

2. Experimental section

The concept of a FPLD filtered EDFL system using a mutually injection-locked EDFL–FPLD link is illustrated in Fig. 1. The configuration originates from the mutually injection-locked DFBLD–EDFL link studied previously, in which the slave laser (EDFL) is forced to synchronously oscillate with the single-mode master laser (DFBLD) [19]. However, the lasing linewidth of master laser can be further shrank due to the precise tuning of the mutually feedback injection from the slave laser [20]. In our case, the master and slave lasers have been changed as the FPLD

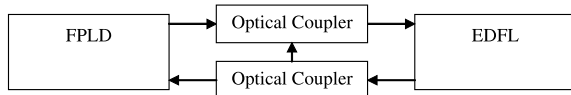


Fig. 1. The concept of a FPLD filtered EDFL based on a mutual injection locking of the EDFL and the FPLD.

and the EDFL, respectively. The configuration of the proposed FPLD filtered EDFL system (illustrated in Fig. 2) consists of a dual-pumped commercial EDFA with maximum power-gain of 21 dBm, a commercial fiber-pigtailed FPLD with central wavelength of 1561 nm at temperature of $35 \text{ }^\circ\text{C}$, an in-line polarization controller (PC), and four optical couplers (OCs) with various power-splitting ratios. Such a design excludes the use of other expansive components such as optical circulators, fiber Bragg gratings, DBR or DFBLDs, and narrow band-pass filters. The combined EDFL–FPLD cavity length is about 50 m, which corresponds to a longitudinal mode spacing of about 4 MHz. In experiments, the OC1 (with splitting ratio 90/10) and OC2 (with splitting ratio 50/50) couple the output of fiber-pigtailed FPLD into EDFL, whereas part of EDFL output is feedback into the FPLD via the use of OC1 and OC4 (with splitting ratio 90/10). The 90% output of EDFL is coupled from OC3 to preserve the saturation of intra-cavity power in EDFL ring cavity. The in-line PC is mandatory for fine-adjusting the polarization and power of the feedback-injecting light to match the eigenstates of FPLD. This arrangement not only guarantees the single-mode oscillation but also suppresses the side-mode induced noise of both the FPLD and

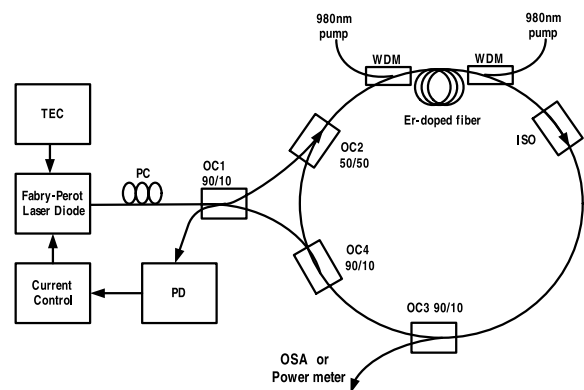


Fig. 2. The experimental setup of single-mode EDFL with intra-cavity feedback-injection FPLD. PC, polarization controller; OC1, 90/10 optical coupler; OC2, 50/50 optical coupler; OC3, 90/10 optical coupler; OC4, 90/10 optical coupler; PD, photodetector; TEC, temperature controller; ISO, optical isolator; OSA, optical spectrum analyzer.

the EDFL at free-running scheme. Under a controlled temperature stability ($\Delta T/T$) of $<1 \times 10^{-3}$, the threshold current and longitudinal mode spacing of the free-running FPLD temperature-controlled at 35°C is about 13.7 mA and 1.02 nm, respectively. The lasing power and spectrum of EDFL with FPLD tuning at different currents and temperatures were measured by using optical spectrum analyzer with resolution bandwidth of 0.01 nm (Advantest, Q8384) and optical power meter (ILX Lightwave, OMM-6810B). The stability of lasing wavelength was further determined by use of a wavelength meter with resolution of 0.001 nm (Advantest TQ8325). The self-heterodyne mode-beating noise and the overall RIN spectra of the FPLD filtered EDFL output ranging from 0 Hz to 2500 MHz (with resolution bandwidth of 1 Hz) are monitored by use of a high-speed photodetector without trans-impedance amplifier (New Focus, 1014) in connection with a Bias-Tee ($f_{3\text{dB}} = 18\text{ GHz}$) and a RF spectrum analyzer (Rhode & Schwartz, $f_{3\text{dB}} = 40\text{ GHz}$).

3. Results and discussion

It is worthy noting that the mutual injection-locking behavior in the proposed FPLD–EDFL link is slightly different from that of the DFBLD–EDFL link ever reported. Both of the lasers are lasing in the DFBLD–EDFL link and the linewidth reduction is dominated by the feedback power injecting into the DFBLD. In contrast, the lasing modes of the EDFL–FPLD link changes abruptly at different driven currents of FPLD due to the exchange of the master and slave roles of these two lasers. As the driven current adjusted far below threshold region, such link is lasing at multiple EDFL longitudinal modes condition. As the driven current tuned close to threshold value within 10% deviation, the EDFL–FPLD link is lasing at a cavity-selected FPLD longitudinal mode (with about 100 EDFL longitudinal modes lasing under the envelope of such a FPLD longitudinal mode). As the driven current becomes larger than threshold, the FPLD mode profile turns to dominate the lasing spectrum of the EDFL–FPLD link. The narrowest linewidth of

such a link can be observed when driving the FPLD at just below threshold condition. This is achieved via the precise control on feedback injecting power from the EDFL to the FPLD, which helps selecting one of the longitudinal modes in the FPLD cavity. Afterwards, the FPLD feedback-injects the EDFL and forces it to oscillate synchronously. Such an operation finally gives rise to a mutually injection-locking between the EDFL and FPLD. It is worth noting that the single FPLD longitudinal mode lasing with linewidth reduction of the EDFL–FPLD link can only be observed by setting the FPLD driven at below threshold condition, which is unavailable to make a free-running FPLD lasing. This is also the most different feature of the EDFL–FPLD link as compared to the EDFL–DFBLD reported previously. Furthermore, the fine tune of the feedback injecting power into the FPLD is also a key procedure in experiment to maintain and stabilize the single FPLD longitudinal mode lasing performance of the EDFL–FPLD link.

Fig. 3 illustrates the power–current characteristics of a free-running FPLD (dashed line) operated at temperature of 35°C and the EDFL (solid line) feedback-injected by the FPLD that functions as an intra-cavity OBPF. It is seen that the EDFL has already been lasing even though FPLD is un-

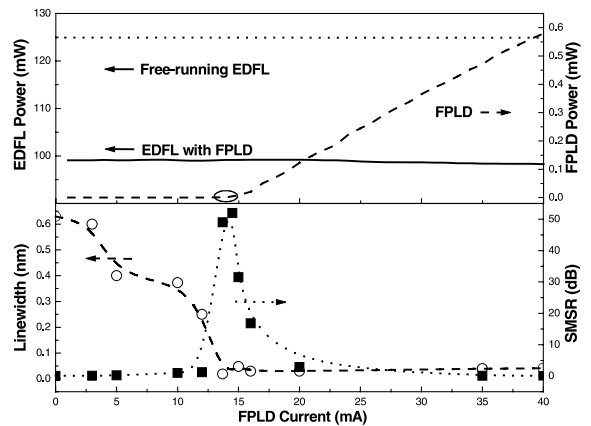


Fig. 3. Upper: the power–current curve of free-running FPLD (dashed line), free-running EDFL (dotted line), and FPLD filtered EDFL (solid line). Lower: the lasing linewidth and SMSR of the FPLD-filtered plotted as a function of FPLD driven current (under the FPLD feedback-injecting power of $12.4\ \mu\text{W}$).

biased, however, the output spectrum of the free-running EDFL is relatively broadened no matter the FPLD is turning off, biasing at well-below threshold condition, or lasing at well-above threshold condition. The former two cases clearly interpret that the filtering ability of FPLD to EDFL is less decisive when operated at such conditions, the EDFL is thus multi-mode lasing at self-seeding mode in these cases. On the contrary, the EDFL acts rather like a close-loop regenerative amplifier (or slave laser) for the FPLD in the latter case. The situation significantly changes as the FPLD biased at nearly threshold current, the linewidth of the EDFL–FPLD link dramatically decreases. One of the amplified longitudinal modes within the correlated gain profile of EDFL and FPLD eventually overcomes the loss of the intra-cavity FPLD operated at just below threshold condition, which turns to dominate the lasing wavelength of the FPLD as well as the EDFL. As a result, the SMSR of the FPLD filtered EDFL system greatly increases to nearly 50 dB associated with its linewidth decreasing to 0.017 nm. This is achieved by driving the FPLD at just below threshold condition under a sufficiently low-feedback injecting power of 12.4 μW , which although helps the single-mode and high-SMSR operation, however, endues some suppression in gain of EDFL. The output power of the EDFL–FPLD link is up to 98.6 mW. Such a narrow-linewidth FPLD filtering procedure only costs 20% (or 1 dB) loss of the EDFL operated at free-running mode (~ 125 mW). The measured power variation of the EDFL is within ± 0.01 mW for 30 min.

The lasing spectra of the free-running FPLD, the EDFL with commercial OBPF, and the FPLD filtered EDFL are illustrated in Fig. 4. Obviously, the free-running FPLD exhibits a relatively wide lasing spectrum with poor signal-to-noise ratio (SNR) of about 20 dB. The 3 dB linewidth and SMSR of the free-running FPLD spectrum are at least 2.2 nm and < 2 dB, respectively. The linewidth of a single longitudinal mode in the free-running FPLD are 0.07 nm. On the other hand, the EDFL with an intra-cavity OBPF exhibits 3 dB lasing linewidth and SNR of 0.36 nm and > 40 dB. In comparison, the measured spectral linewidths of the FPLD filtered EDFL are 0.017 nm

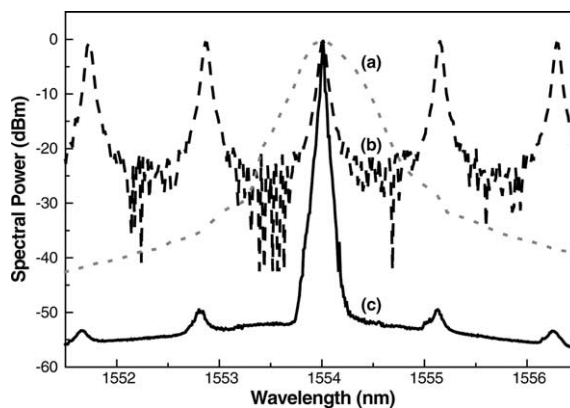


Fig. 4. The lasing spectra of free-running FPLD (dashed line), the EDFL filtered with an intra-cavity commercial OBPF (dotted line), and FPLD filtered EDFL (solid line) with the feedback-injected FPLD biasing at just below threshold.

(corresponding to 2.37 GHz) and 0.042 nm at 3- and 10-dB decay, respectively. The optimized SMSR and SNR of the FPLD filtered are up to 50 and 54 dB, respectively. The short-term fluctuation of SMSR is less than ± 0.5 dB at measuring duration of 10 min. It is seen that the linewidth of the lasing spectrum from the EDFL–FPLD link ($\Delta\lambda_{3\text{dB}} < 0.017$ nm) is far smaller than those of free-running EDFL or EDFL with commercial OBPF, and is even smaller than that of a longitudinal mode in free-running FPLD. This is mainly attributed to the mutual injection-locking mechanism in such link. These results clearly illustrate that the proposed EDFL–FPLD system could probably exhibit a narrow-linewidth or even a single-mode spectrum which has already beyond the systematic resolution. To confirm, the self-heterodyne mode-beating spectrum of the EDFL–FPLD link with FPLD biasing at just below and above threshold currents have been measured, as shown in Fig. 5. The beating mode spacing of about 4 MHz corroborates the longitudinal mode spacing evaluated previously. It is observed that the EDFL–FPLD link did not generate a single EDFL longitudinal mode lasing in the combined cavity even at just below threshold condition. The beating spectral bandwidth at 10- and 20-dB decay of the EDFL–FPLD link are about 60 and > 100 MHz, respectively. The corresponding linewidths are estimated as 0.5 and 0.8 pm. The beating

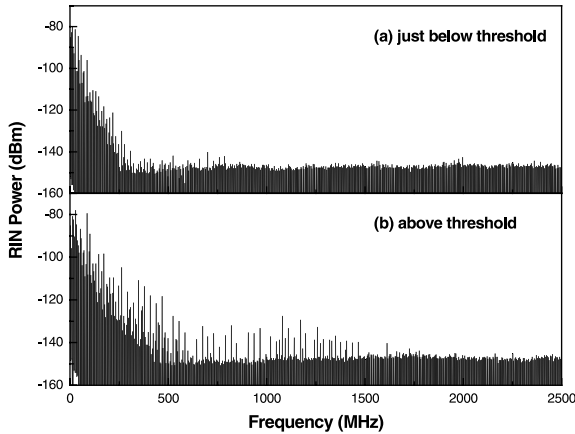


Fig. 5. The comparison on the self-heterodyne mode-beating spectra of the FPLD filtered EDFL with the FPLD operating at just below and above threshold conditions.

spectrum of the EDFL–FPLD link further extends to 1.5 GHz as the driven current of the FPLD increases to above threshold. The degradation in mode-beating spectrum results from the grown-up of other FPLD side-modes in the FPLD filtered EDFL. Furthermore, the RIN spectrum of the FPLD filtered EDFL is also characterized and compared with that of a DFBLD (see Fig. 6). The overall RIN of the DFBLD (thermal and shot noises of the measurement included) rapidly decays to -145 dBm/Hz background at frequency beyond 50 MHz. The RIN of EDFL–FPLD link linearly decreases from -80 dBm/Hz to background within 300 MHz bandwidth.

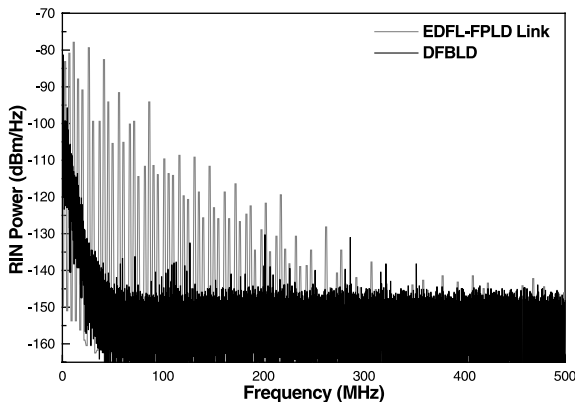


Fig. 6. The comparison on the RIN spectra of the DFBLD and the FPLD filtered EDFL.

By fine-tuning the driven current of FPLD at a specified temperature, the output wavelength of the FPLD filtered EDFL can be adjusted from 1557.5 to 1563.5 nm as the temperature of FPLD adjusts from 10 to 50 °C, as shown in Fig. 7. This is demonstrated by using another FPLD with central wavelength of 1558.7 nm at free-running mode. The variance in output power and lasing wavelength are ± 0.01 mW and ± 0.025 nm, respectively. Experimental results also reveal that either the increasing in dc bias (or decreasing in operating temperature) may not only lead to broadening of spectral linewidth, but also causes a red shift in the lasing wavelength of EDFL. For example, Fig. 8 illustrates the output optical spectra of the EDFL with intra-cavity FPLD driven at different current conditions (below, near, and above threshold current) and operated temperature at 35 °C. The degradation in the spectral linewidth of EDFL is inevitable since the threshold current of the FPLD at different temperatures is also varied. However, the shift in spectral range of the feedback-injected FPLD caused by both the change in density and energy distribution of carriers is slightly larger than that of a free-running FPLD. In addition, the broadened output spectra with multiple side-modes and worse SMSR due to the lasing of the unexpected longitudinal modes in the commercial FPLD driven at same biased current but different temperatures can also be obtained (see Fig. 9). This again corroborates the effect of FPLD on the side-mode suppression of

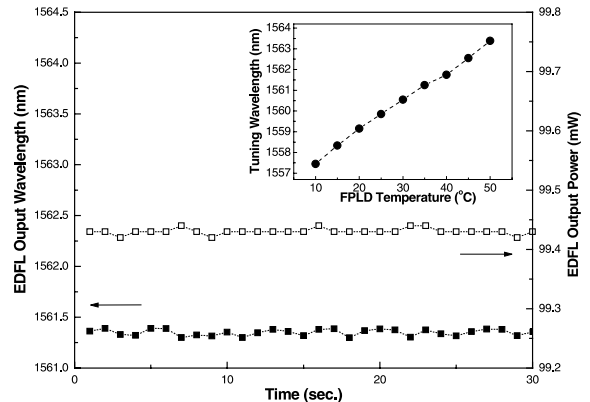


Fig. 7. The wavelength tunability and the long-term stabilities in output power and lasing wavelength of FPLD filtered EDFL.

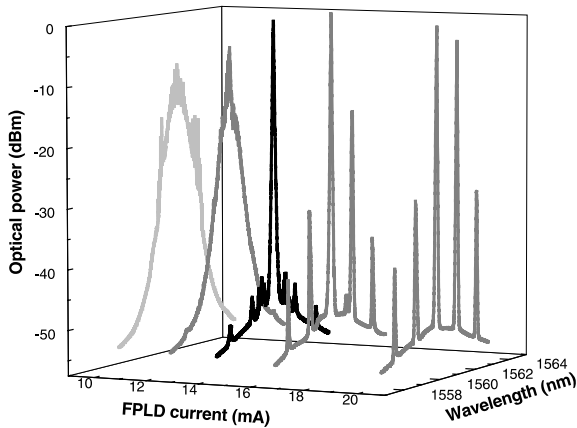


Fig. 8. The measured spectra of the FPLD filtered EDFL with the feedback-injected FPLD (at constant temperature of 35 °C) biased at different current condition.

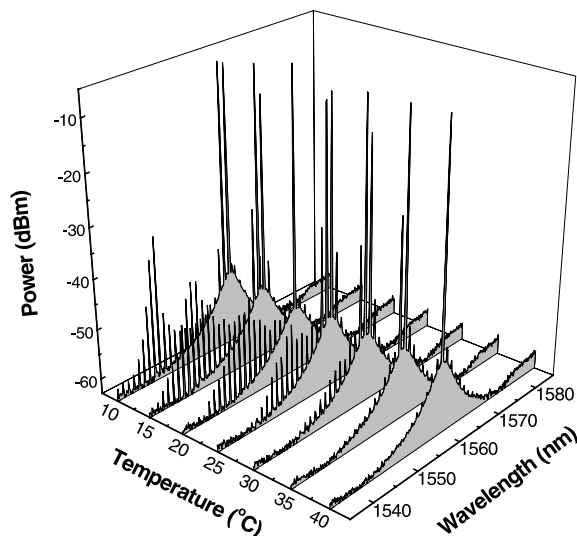


Fig. 9. The degraded lasing spectra of the FPLD filtered EDFL (biased at constant current of just below threshold at 40 °C) at different operating temperatures of FPLD.

the EDFL since that the same bias current may already exceed the threshold of the FPLD operated at lower temperatures. However, the peak wavelength of the EDFL is still predominated by one of the overlapped modes in the convoluted gain profile of the EDFL and FPLD [21]. This is another striking feature of the proposed system, that is, the tuning resolution of the lasing wavelength can be much smaller than the longitudinal mode spacing of the FPLD due to the long-cavity of the EDFL. Therefore, it is realized that even the free-running FPLD is operated at nearly lasing region, the broadband spontaneous emission spectrum of the FPLD reveals that there is still a competition between cavity modes results from spontaneous emissions. At this stage, even a small intra-cavity feedback power can efficiently lead to the survival of one mode in cavity, which eventually suppresses the lasing of other modes in both the FPLD and EDFL [22]. The narrow-linewidth operation and mode-selection of the EDFL is therefore achieved by fine-tuning the power ($\sim 0.01\%$ from the EDFL output at TE mode in optimized case) and polarization of the feedback-injected light into FPLD. The performances of the proposed FPLD filtered EDFL in comparison with free-running FPLD, free-running EDFL, EDFA-amplified FPLD, and EDFL with OBPF are summarized in Table 1. To date, we take the advantages of mutual injection locking technique to demonstrate a novel approach of narrow-linewidth and wavelength tunable EDFL source. Instead of using a FPLD as an actively tunable and high-finesse band-pass filter, no other spectral-confined and wavelength-selective components such as FBG or high-finesse FPF are employed. Such a configuration has shown to be relatively stable under precise control of the FPLD temperature. The simple and low-cost design has made

Table 1

The comparison in output characteristics of different FPLD-based or EDFL-based laser schemes

	SMSR (SNR)	Output power (mW)	Spectral (mode) linewidth	Loss
FPLD free-running	<2 dB (~ 20 dB)	10s	2.2 nm (0.07 nm)	–
FPLD–EDFA	<2 dB (~ 20 dB)	140	2.2 nm (0.07 nm)	–
EDFL free-running	– (30–35 dB)	125	1.35 nm (–)	–
EDFL with OBPF	– (>40 dB)	75	0.36 nm (–)	2–2.5 dB
EDFL–FPLD link	~ 50 dB (54 dB)	99	0.017 nm (–)	0.9–1 dB

the proposed EDFL very promising for versatile applications in the near future.

4. Conclusions

In conclusion, we demonstrate a novel approach for obtaining narrow linewidth EDFL with ultrahigh SMSR by adding a FPLD into the EDFL ring cavity (connecting by commercial optical couplers) and feedback-injection the FPLD with part of the EDFL output via polarization controller. To help selecting the strongest mode from the gain-spectrum of FPLD for lasing in the EDFL ring cavity, the FPLD biased at just below threshold condition with operating temperature of 35 °C is employed as an active OBPF. The lasing wavelength of EDFL is controlled by both the gain profiles of EDFA and FPLD, however, the effect of FPLD longitudinal mode is found to be more pronounced at its driven current close to threshold. With this technique, the spectral widths at 3- and 10-dB decay are as small as 0.017 and 0.042 nm, respectively. Ultrahigh SMSR and SNR of up to 50 and 54 dB are observed, respectively. The variations in output power, SMSR, and lasing wavelength are ± 0.01 mW, ± 0.5 dB, and ± 0.025 nm, respectively. The narrow linewidth EDFL still provides average power of up to 99 mW at a dissipation of 1 dB. Such a scheme successfully combines the high-power characteristic of EDFL and the mode-selecting and tuning capability of the FPLD via the mutual injection-locking technique. The use of intra-cavity FPLD based filter further benefits from advantages such as low-cost, stable, simple design, and compact size as compared to the conventional approaches.

Acknowledgements

This work was supported in part by the National Science Council (NSC) of the Republic of China under grant NSC91-2215-E-009-039.

References

- [1] G. Morthier, P. Vankwikelberge, *Handbook of Distributed Feedback Laser Diodes*, Artech House, Boston, 1997 (Chapters 1–3).
- [2] Y. Zhao, C. Shu, *IEEE Photon. Technol. Lett.* 9 (1997) 1436.
- [3] J.L. Zyskind, J.W. Sulhoff, Y. Sun, J. Stone, L.W. Stulz, G.T. Harvey, D.J. Digiiovanni, H.H. Presby, A. Piccirilli, U. Koren, R.M. Jopson, *Electron. Lett.* 27 (1991) 2148.
- [4] S. Kobayashi, J.Y. Yamada, S. Machida, T. Kimura, *Electron. Lett.* 14 (1980) 746.
- [5] K. Iwashita, K. Nakagawa, *IEEE J. Quantum Electron.* QE-18 (1982) 1669.
- [6] C. Lin, J.K. Andersen, F. Mengel, *Electron. Lett.* 21 (1985) 80.
- [7] M. Schell, W. Utz, D. Huhse, J. Kassner, D. Bimberg, *Appl. Phys. Lett.* 65 (1994) 3045.
- [8] S. Li, K.S. Chiang, W.A. Gambling, Y. Liu, L. Zhang, I. Bennion, *IEEE Photon. Technol. Lett.* 12 (2000) 1441.
- [9] Y.K. Sin, Y. Qiu, R.E. Muller, S. Forouhar, *Electron. Lett.* 37 (2001) 567.
- [10] T. Ogawa, *IEEE J. Quantum Electron.* QE-25 (1989) 2169.
- [11] G.A. Ball, W.W. Morey, W.H. Glenn, *IEEE Photon. Technol. Lett.* 3 (1991) 613.
- [12] G.A. Ball, W.W. Morey, *Opt. Lett.* 17 (1992) 420.
- [13] J.L. Zyskind, V. Mizrahi, D.J. Digiiovanni, J.W. Sulhoff, *Electron. Lett.* 28 (1992) 1385.
- [14] V. Mizrahi, D.J. Digiiovanni, R.M. Atjins, S.G. Grubb, Y.-K. Park, J.-M.P. Delavaux, *J. Lightwave Technol.* 11 (1993) 2021.
- [15] N. Park, D.J. Dawson, K.J. Vahala, C. Miller, *Appl. Phys. Lett.* 59 (1991) 2639.
- [16] K. Petermann, *Laser Diode Modulation and Noise*, Kluwer, London, 1988 (Chapter 4).
- [17] J. Zhang, C.Y. Yue, G.W. Schinn, W.R.L. Clements, J.W.Y. Lit, *J. Lightwave Technol.* 14 (1996) 104.
- [18] M. Schell, D. Huhse, A.G. Weber, F.G. Bimberg, D.S. Tarasov, A.V. Gorbachov, D.Z. Garbuzov, *Electron. Lett.* 28 (1992) 2154.
- [19] L.W. Liou, M. Yu, T. Yoshino, G.P. Agrawal, *Electron. Lett.* 31 (1995) 41.
- [20] S. Saito, Y. Yamamoto, *Electron. Lett.* 17 (1981) 325.
- [21] D. Zhao, K.L. Li, K.T. Chan, H.-F. Liu, *Electron. Lett.* 36 (2000) 1700.
- [22] D.-S. Seo, H.-F. Liu, D.Y. Kim, D.D. Sampson, *Appl. Phys. Lett.* 67 (1995) 1503.
- [23] S. Li, K.S. Chiang, W.A. Gambling, *IEEE Photon. Technol. Lett.* 13 (2001) 1364.